

331. Analysis of the Dynamics of the Vibratory Valve-Injector

V. Naginevicius^{1,a}, M. Ragulskis^{2,b} and A. Palevicius^{3,c}

Kaunas University of Technology,

Kestucio 27-217, LT-44312, Kaunas, Lithuania

E-mail: ^avytenis.naginevicius@ktu.lt, ^bminvydas.ragulskis@ktu.lt, ^caryvydas.palevicius@ktu.lt

(Received 19 January 2008; accepted 17 March 2008)

Abstract. Construction of a novel vibratory valve-injector and its design optimization is presented in the paper. The principle of the system operation is based on the effect of dynamic positioning of a steel ball in a vibrating tube. Theoretical analysis of the stability of this non-linear system is coupled together with the experimental study of an operating valve. Laser holographic interferometry is used for the identification and optimization of working regimes of the system.

Keywords: Vibratory valve, injector, mathematical modeling, holographic interferometry, fluid dynamics

Introduction

Controlled dosing and spraying of liquid material is applied in different areas ranging from medicine to agriculture [1], [2]. Specific interest exists for elastic catheter pipe type dosing equipment. Complex dynamic processes taking place in such systems are analyzed in [3], [4]. Method examining the dynamic characteristics of a tube under the influence of the internal flow is presented in [3]. Galerkin's method in conjunction with the method of multiple scales is employed for obtaining the stability of the tube vibration. According to the results, instability can occur under certain conditions of resonance. In [4] it is demonstrated that fluid-elastic effects which are responsible for fluid-elastic instabilities may be directly measured through the analysis of the vibrating motion of a system under flow. Piezoelectric actuators are used to increase the vibratory level when buffeting forces which excite tube vibration are low, and to improve the measurement of fluid-elastic forces.

Application of piezoelectric actuators for the generation of standing waves in the outlet pipe can produce effects which can be exploited for the control of the dosing process. The motion of fluid-suspended particles and fibers in a standing wave field is analyzed in [5], [6]. The dynamics of micron-sized aerosol particles and their agglomeration under the standing wave conditions is analyzed in [7]. Coupling of the dynamic properties of a vibrating tube with the dynamic behavior of a steel ball inside that tube can help producing a new type of smart doser for liquid material which can be

effectively controlled by piezoelectric actuators. The unique feature of the tubular vibratory valve consists in the fact that the sealing surface of the seat is facing towards the intake duct and is located in the node of the second natural mode of transverse vibration of the elastic pipe. The vibratory valve for controlling liquid flow 1 (Fig. 1) operates in the following way.

Several versions of design of systems for fluid flow control are presented in the following diagrams.

A. The fluid flow controller is presented in Fig. 1.

The controller is composed of tube (1) with input (2) and output (3) channels. A valve consisting from the closing element 5, spring 4 and seat 6 is mounted inside the tube. Vibration exciter 7 is fixed to the one end of the tube. Limiter 9 is placed inside the rigid tube 8 which is fastened to membrane 10. The surface of the tube from the seat 6 up to limiter 9 is cone shape. The feeding generator 11 is controlling the vibrator.

The spring 4 presses the limiter 5 into the seat 6 and shuts the flow in the tube when the vibration exciter is off. Standing waves are excited in the tube when the vibrator is on. The excitation frequency coincides with the natural frequency of the system and the fluid flow controller operates in the resonance mode. That enables to reach higher amplitudes and the limiter 5 moves against the spring force into the peak of standing wave and thus opens the fluid flow channel.

B. Fluid sprayer.

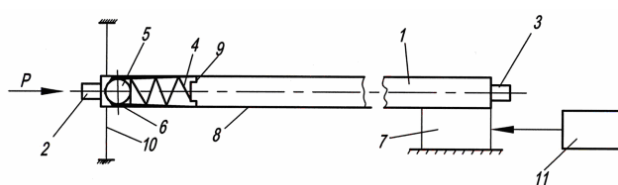


Fig. 1. Schematic diagram of fluid flow controller

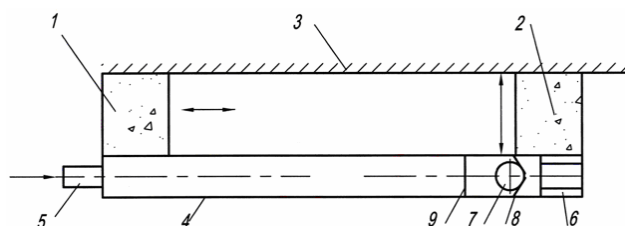


Fig. 2. Schematic diagram of the vibration sprayer

The vibration sprayer (Fig. 2) consists of longitudinal (1) and transverse (2) vibration generators attached to the motionless foundation 3; tube 4 with input (5) and output (6) channels. Limiter 7 and seat 8 are mounted inside the tube. Fluid pressure pushes the limiter 7 into the seat 6 when the vibrator is off. Standing waves are generated in the tube 4 when the vibrator 2 is on. The limiter moves into the peak of the standing wave and opens the fluid valve.

The fluid is sprayed by the oscillating end (6) of the tube (Fig. 3a). The eigenshape of the tube end (6) when the vibrator 1 is switched on. The standing wave length is shortened and the limiter is pressed into the seat – the spraying process is stopped. Such control mode enables reaching higher control frequencies compared to the control method used in Fig. 1.

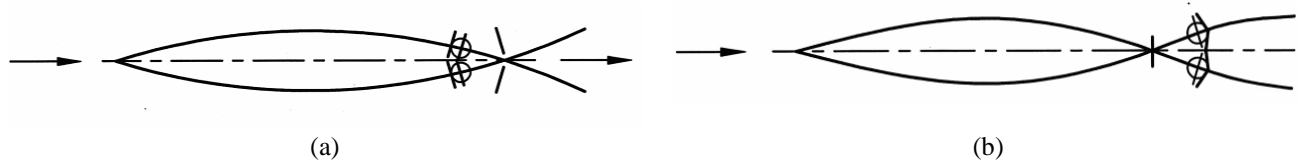


Fig. 3. Operation diagram of the vibration sprayer: a) valve is open; b) valve is closed

C. Vibration fluid doser (Fig. 4).

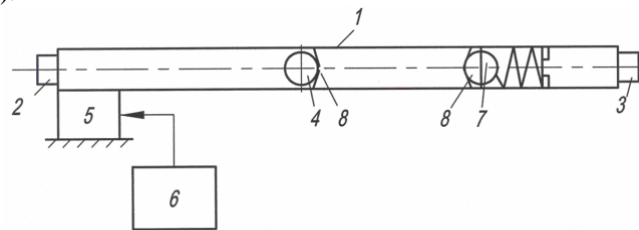


Fig. 4. Schematic diagram of the vibration fluid doser

Vibration fluid doser consists from chamber 1 with input (2) and output (3) channels, electromechanical drive 5, controller 6, secondary valve 7 which is pressed by the spring to one of the seats. The chamber is a rigid tube, electromechanical drive serves as an exciter of transient vibrations. The placement of the first (4) and the secondary (7) valves defines the operating principle of the doser. The fluid flows through the input channel and closes the first valve when the vibrator 5 is off. The vibrator excites the third eigenshape vibrations (two standing waves) in the

process of fluid dose formation. The valve 4 opens, but the secondary valve 7 closes (Fig. 5a). Next, the second eigenshape vibrations are generated (Fig. 5b). The first valve 4 gets closed, the secondary valve is still kept closed. The formation of the dose is finished. The dose is ejected when the first eigenshape vibrations are generated (Fig. 5c). The first valve is kept closed, but the secondary valve is opened.

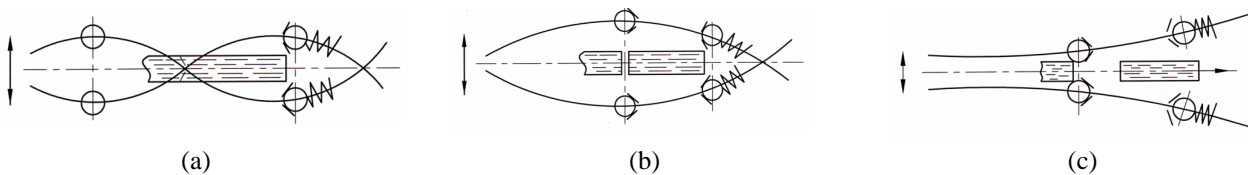


Fig. 5. Operation principle of the vibration fluid doser: a, b and c – the three stages of the doze formation

Dynamics of a steel ball inside a vibrating tube

Motion of a small ball inside a tube performing transverse vibrations may be approximated by the non-dimensional

differential equation of motion describing the dynamics of a mass particle on an oscillating profile with an obligatory condition of contact with the surface [3], [4]:

$$\left(1 + \left(\frac{\partial \zeta}{\partial x}\right)^2\right) m \ddot{x} + \frac{\partial^2 \zeta}{\partial x^2} \frac{\partial \zeta}{\partial x} m (\dot{x})^2 + 2 \frac{\partial^2 \zeta}{\partial x \partial t} \frac{\partial \zeta}{\partial x} m \dot{x} + h \left(1 + \left(\frac{\partial \zeta}{\partial x}\right)^2\right) \dot{x} + \frac{\partial^2 \zeta}{\partial t^2} \frac{\partial \zeta}{\partial x} m + \frac{\partial \zeta}{\partial x} mg = F, \quad (1)$$

where $\zeta = \zeta(x, t)$ – the shape of the tube; x, \dot{x}, \ddot{x} – projections of the displacement, velocity and acceleration of the ball onto the horizontal axis; t – time; m – mass of the ball; h – the coefficient of viscous friction between the ball and the surface of the profile; g – the acceleration of gravity; F – the pressure force of the liquid.

Naturally, Eq.(1) is based on the assumption that the area of the cross section of the tube is small, the fluid flow is laminar, and the pressure of the liquid in the tube does not correlate with the amplitude of the elastic transverse vibrations. Also it is assumed that the mass of the locking ball is sufficient enough to perform the vibration induced motion in the liquid, but not big enough to alter the shape of the tube's vibration due to its relocation.

Such mathematical model of the system enables effective separation of ball's motion to relatively fast and slow motions. Co-ordinate x represents the horizontal displacement of the ball (slow motion), while the motion of the ball in the vertical direction is defined by the function $\zeta = \zeta(x, t)$.

When the tube performs steady oscillations of a standing wave type, the form of the tube looks like:

$$\zeta(x, t) = b \cos(kx) \cos(\omega t), \tag{2}$$

where b – the amplitude of oscillations, k and ω – the number and frequency of the standing wave respectively.

When the vibrations take place in the horizontal plane xOy (Fig. 1) and no external force is applied to the mass particle, the following conditions are satisfied:

$$\begin{aligned} g &= 0, \\ F_x &= 0, \\ \dot{x} = \ddot{x} &= 0, \end{aligned} \tag{3}$$

Then, the condition of existence of the steady state solutions is found from Eq. (1):

$$\frac{\partial^2 \zeta}{\partial t^2} - \frac{\partial \zeta}{\partial x} = 0, \tag{4}$$

or applying Eq. (2) to Eq. (4) :

$$x = \frac{\pi}{k} \cdot s, \quad s \in Z, \tag{5}$$

and

$$x = \frac{\pi}{2k} + \frac{\pi}{k} \cdot s, \quad s \in Z \tag{6}$$

Analogously, if the vibrations take place in the vertical plane xOz (Fig. 1), and no external force is applied to the mass particle, the condition of existence of the steady state solutions looks like:

$$\frac{\partial^2 \zeta}{\partial t^2} - \frac{\partial \zeta}{\partial x} + \frac{\partial \zeta}{\partial x} g = 0, \tag{7}$$

or

$$x = \frac{\pi}{k} s, \quad s \in Z. \tag{8}$$

If the external force is non-zero, there are no steady state solutions satisfying the condition $\dot{x} = \ddot{x} = 0$.

Stability of solutions when the vibrations take place in the horizontal plane

The stability of the solution described by Eq. (5) is checked constructing the variational equation around $x = \frac{\pi}{k} \cdot s$ using the following assumption:

$$x = \frac{\pi}{k} s + dx, \tag{9}$$

here dx is a small variation about the steady state solution. After the assumption of approximations

$$\begin{aligned} \sin\left(k\left(\frac{\pi}{k}s + dx\right)\right) &\approx \sin(\pi s) + \cos(\pi s) \cdot kdx = (-1)^s kdx \\ \cos\left(k\left(\frac{\pi}{k}s + dx\right)\right) &\approx \cos(\pi s) - \sin(\pi s) \cdot kdx = (-1)^s \end{aligned} \tag{10}$$

and rejection of terms with $(dx)^2$ and $(dx)^3$, the following variational equation is produced from Eq. (1):

$$md\ddot{x} + hd\dot{x} + (bkw \cos(\omega t))^2 dx = 0. \tag{11}$$

Since all coefficients of this ordinary differential equation are positive in the neighborhood of t , the real parts of both roots of the characteristic equation will be negative. Thus the solution of the variation is stable and the position $x = \frac{\pi}{k} + dx$ is also stable. The value of the discriminant of the characteristic equation of Eq. (11) will define the type of the stable attractor. Averaging in time produces the following equation:

$$d\ddot{x} + \frac{h}{m}d\dot{x} + \frac{(bkw)^2}{2m}dx = 0. \tag{12}$$

Therefore, the stable attractor will be of a knot type and the roots of the characteristic equation of Eq. (12) will be real, i.e. the discriminant is positive, and the attractor of the

focus type when the roots are complex (discriminant is negative). That produces the following relations:

- a) the attractor of the knot type at $b \leq \frac{h}{mwk}$;
- b) the attractor of the focus type at $b > \frac{h}{mwk}$.

The stability of the solution described by Eq. (6) is checked in analogous way:

$$x = \frac{\pi}{2k} + \frac{\pi}{k}s + dx, \tag{13}$$

here dx is a small variation. Rejection of the non-linear terms and the following approximations

$$\begin{aligned} \sin\left(k\left(\frac{\pi}{2k} + \frac{\pi}{k}s + dx\right)\right) &\approx (-1)^s \\ \cos\left(k\left(\frac{\pi}{2k} + \frac{\pi}{k}s + dx\right)\right) &\approx -(-1)^s kdx \end{aligned} \tag{14}$$

in Eq. (1) lead to:

$$\begin{aligned} (1 + k^2 b^2 (\cos wt)^2) m d\ddot{x} + \\ (-mk^2 b^2 w \sin 2wt + h(1 + k^2 b^2 (\cos wt)^2)) d\dot{x} - \\ w^2 b^2 k (\cos wt)^2 m dx = 0 \end{aligned} \tag{15}$$

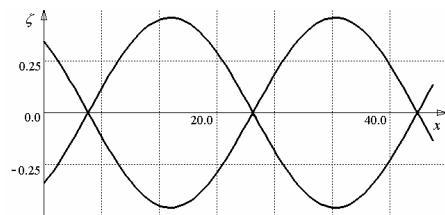
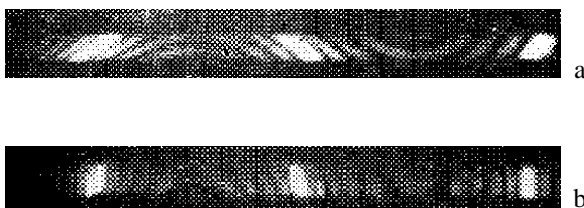
The coefficient of this ordinary differential equation at dx is negative in entire neighborhood of the local time t . Thus, at least one of the roots of the characteristic equation Eq.(15) will be positive, and the solution in Eq.(13) will be unstable. Thus, the positions of the ball at the nodal points of the vibrating profile are unstable. Alternatively, the positions at the peaks of the profile, i.e. at the points which vibrate with the maximum amplitude, are stable. Of course, that is true when the ball cannot jump off the surface of the profile (is placed inside a vibrating tube).

Experimental Analysis of a Tubular Vibratory Valve

A number of experimental studies are needed in order to ensure high dynamic accuracy of operation of the vibrator

valves for controlling the flow of liquid substances. In most cases the exciting frequencies of the tubular working tube are fairly high, and the amplitudes corresponding to them are measured in micrometers. Therefore the holographic method can be effectively applied for the visual representation of wave processes taking place in the tubular vibratory valve ([1], [2]). The most effective method for studying the standing wave processes is the method of holographic interferometry with time averaging ([5], [6]). It should be noted that the most clearly expressed bands in the holographic interferograms are those recorded at the positions of minimum amplitudes ([7]). It is important to obtain the distribution of the vibration amplitudes not only in the middle of dark interference bands, but also in arbitrary positions on the surface of the tube. That enables the determination of the location of the steel ball inside the tubular valve. The amplitudes of vibration of the structure are determined using the methodology presented in [8], [9]. Holographic interferograms of the transverse vibrations of a tubular vibratory valve are presented in Fig. 6a, Fig. 6b and Fig. 7a. Fig. 6a and Fig. 6b make it possible to conclude that transverse vibration of the tube is sufficiently uniform (Fig. 6c). Therefore, the seat of the vibratory can be located in a nodal point, regardless of how it is displaced lengthwise in the upper or the lower nodal point of the tube. It should be noted that the frequency of excitation must be selected with care since the best performance of the vibratory valve is taking place at the resonant frequencies. If the excitation of the transverse vibrations is far away from the resonance frequencies of the tube, the operation of the tubular valve turns to be hardly controlled.

The obtained results enable to optimize the design of the vibratory valves for controlling and dosing the liquid flow. The following parameters of the system are analyzed and optimized: a) selection of the material of the working tube; b) selection of the area of the transverse cross section of the tubular tube; c) location of the transverse vibration nodes in the tube; d) determination of the transverse vibration amplitudes along the tube. Maximum uniformity of the transverse vibrations in the vibratory valve is achieved due to this optimization which leads to more stable operation of the whole system.



a. The hologram of the transverse vibrations of the tube at $w = 1,3$ kHz. Illumination angle of the laser beam $\pi / 4$; 6b. The hologram of the tube at the illumination angle $\pi / 2$

c. The interpretation scheme of the transverse vibrations

Fig. 6. Holographic interferogram of transverse vibrations of the tube

Concluding Remarks

New model of a tubular vibratory valve is designed using the stabilization effect of a steel ball in the vibrating tube. The methodology of identification of vibration peaks enabled experimental optimization of the working regimes of the system. Such type of analysis could be successfully applied in the design stage of different precise vibratory systems.

References

- [1] **Cho K. J. and Recinella, D. K.** Pattern of dispersion from a pulse-spray catheter for delivery of thrombolytic agents: Design, theory, and results, *J. Academic Radiology*, 4(3), 210-216, (1997)
- [2] **Miller P. and Ellis M.** Effects of formulation on spray nozzle performance for applications from ground-based sprayers, *J. Crop Protection*, 19(8-10), 609-615, (2000)
- [3] **Huang Y. and Hsu C.** Dynamic behavior of tubes subjected to internal and external cross flows, *J. Shock and Vibration*, 4(2), 77-91, (1997)
- [4] **Caillaud S. and de Langre E.** The measurement of fluidelastic effects at low reduced velocities using piezoelectric actuators, *J. of Pressure Vessel Technology – Transactions of the ASME*, 121(2), 232-238, (1999)
- [5] **Brodeur P.** Motion of fluid-suspended fibres in a standing wave field, *J. Ultrasonics*, 29, 302-307, (1991)
- [6] **Coakley W. T. and Zamani F.** Cell Manipulation in ultrasonic standing wave fields. *J. of Chemical Technology and Biotechnology*, 44(1), 43-62, (1989)
- [7] **Riera-Franco de Sarabia E. and Gallego-Juarez J. A.** Ultrasonic agglomeration of micron aerosols under standing wave conditions, *J. of Sound and Vibration*, Palevicius, A., and Ragulskis, M., Holographic interference method for investigation of wave transport systems, *SPIE Proc. of the 2-nd Intl. Conf. on Vibration Measurements by Laser Techniques*, Ancona, Italy, 225-231, (1996)413-427, (1986)
- [8] **Vest C.** *Holographic Interferometry*, Moscow, Mir, (1982)
Palevicius, A., and Ragulskis, M., Holographic interference method for investigation of wave transport systems, *SPIE Proc. of the 2-nd Intl. Conf. on Vibration Measurements by Laser Techniques*, Ancona, Italy, 225-231, (1996) ly, 225-231, (1996)